FUNGAL BIOLOGY XXX (2016) 1–13

British Mycological Society promoting fungal science

journal homepage: www.elsevier.com/locate/funbio

Putative origins of the fungus *Leptographium procerum*

Stephen J. TAERUM[a,b,*], *Thierry B. HOAREAU*[c], *Tuan A. DUONG*[a], *Z. Wilhelm DE BEER*[d], *Robert JANKOWIAK*[e], *Michael J. WINGFIELD*[a]

[a]*Department of Genetics, Forestry and Agricultural Biotechnology Institute (FABI), University of Pretoria, Pretoria 0002, South Africa*
[b]*China Eucalypt Research Centre, Chinese Academy of Forestry, Zhanjiang 524022, China*
[c]*Molecular Ecology and Evolution Programme, Department of Genetics, University of Pretoria, Pretoria 0002, South Africa*
[d]*Department of Microbiology and Plant Pathology, Forestry and Agricultural Biotechnology Institute (FABI), University of Pretoria, Pretoria 0002, South Africa*
[e]*Institute of Forest Ecosystem Protection, Department of Forest Pathology, Mycology and Tree Physiology, University of Agriculture in Krakow, Al. 29 Listopada 46, 31-425 Kraków, Poland*

ARTICLE INFO

Article history:
Received 16 June 2016
Received in revised form
15 September 2016
Accepted 28 September 2016
Corresponding Editor:
Kerry O'Donnell

Keywords:
Dendroctonus valens
Forestry
Invasion biology
Ophiostomatoid fungus
Symbiosis

ABSTRACT

Appropriate management of invasive fungi requires adequate understanding of their global diversities and movement histories. The fungus *Leptographium procerum* is associated with root-colonizing forest insects in pine forests throughout the world, and may have contributed to the aggressive behaviour of the red turpentine beetle (*Dendroctonus valens*) in the beetle's invasive range in China. We used microsatellites and mating type loci to investigate the global diversity of *L. procerum* and the source population of *L. procerum* associated with *D. valens* in China. Clustering analyses supported the separation of the fungal data set into three genetically and geographically-distinct clusters: Europe, North America, and China. The fungus had the highest genetic diversity in Europe, followed by North America and China. Analyses using Approximate Bayesian Computation supported Europe as the most likely source of the North American and Chinese populations. Overall, the results suggested that Europe is the global centre of diversity of *L. procerum*. Furthermore, they suggested that *L. procerum* most likely arrived in China independently of *D. valens* and adopted this beetle as a vector after its introduction.

Introduction

Rising global trade and travel combined with changing environmental conditions have resulted in an increased movement of fungi around the world (Palm 2001; Fisher & Garner 2007; Loo 2009). Invasive fungi have been understudied relative to invasive plants and animals, despite the considerable negative effects of some fungi on invaded environments (Gladieux *et al.* 2014). For example, the tree pathogens *Cryphonectria parasitica* and *Ophiostoma novo-ulmi* dramatically

* *Corresponding author*. Forestry and Agricultural Biotechnology Institute (FABI), University of Pretoria, Private bag X20, Hatfield 0028, South Africa. Tel.: +27 124205821; fax: +27 124203960.
E-mail address: Stephen.Taerum@fabi.up.ac.za (S.J. Taerum).
http://dx.doi.org/10.1016/j.funbio.2016.09.007
1878-6146/

changed forest structure in various parts of the world where they have killed large numbers of chestnuts and elms respectively (Loo 2009). In addition, the global spread of *Puccinia graminis*, a rust fungus that devastates cereal crops, has led to major crop losses in several locations (Palm 2001; Wanyera *et al.* 2006). More recently, the chytrid *Batrachochytrium dendrobatidis* has decimated amphibian populations around the world (Fisher & Garner 2007). Some fungi that are not pathogens in their native ranges have become problematic subsequent to their becoming invasive (Hulcr & Dunn 2011), suggesting that any exotic fungus is potentially damaging and therefore worth monitoring.

Ironically given their global relevance, the impacts of most invasive fungi are poorly understood because they are difficult to observe in the absence of substantial negative effects on the environment (Gladieux *et al.* 2014). Difficulties associated with conducting meaningful fungal surveys along with incorrect knowledge of whether a population of a pathogen is native or invasive can and has resulted in inaccurate conclusions regarding the movement histories of invasive pathogens, and by extension improper management strategies for the organisms (Estoup & Guillemaud 2010; Gladieux *et al.* 2014).

Accidental introductions of invasive fungi are often facilitated by animal vectors. Tree-colonizing insects are especially important vectors because several fungal species depend on these insects for dispersal as well as access to new host trees (Klepzig *et al.* 2009). If a species of tree-colonizing insect undergoes a range expansion or is introduced to a non-contiguous habitat, it can vector its fungal symbionts to environments in which they did not previously occur. In addition, introduced fungi sometimes undergo vector and host shifts, resulting in new associations between tree hosts, insect vectors, and fungal symbionts (Wingfield *et al.* 2010).

Invasions by fungal associates combined with vector and host shifts can have unpredictable, and sometimes serious, impacts on forest health (Ploetz *et al.* 2013; Wingfield *et al.* 2016). For example, some fungi have strong effects on the fitness of damaging tree-colonizing insects (Klepzig *et al.* 2009). Some phoretic fungi are mutualists of their insect associates (e.g., nutritional mutualists; Mueller *et al.* 2005), while others are antagonists (e.g., fungi that compete for substrates with their insect vectors; Cardoza *et al.* 2006). If the fungi are vectored by especially aggressive forest insects, the abundance of these fungi can greatly influence the frequency and intensity of insect outbreaks (Raffa *et al.* 2008). In addition, some phoretic fungi are serious pathogens of trees (Hulcr & Dunn 2011), in some cases causing more damage than their insect vectors.

The symbiosis between the fungus *Leptographium procerum* (Ophiostomatales, Ascomycota) and its vectors provides a model to study the global movement of an invasive fungus, as well as the interactions between invasive fungi, tree-colonizing insects, and invaded environments. *Leptographium procerum* is an ophiostomatoid (defined by Wingfield *et al.* 1993) fungus associated with various bark beetles and weevils (Coleoptera: Scolytinae) that typically infest conifers and especially the roots of *Pinus* spp (Jacobs & Wingfield 2001; Jankowiak *et al.* 2012). The fungus is also vectored by some cerambycid beetles (Coleoptera: Cerambycidae) that feed on roots and stumps of *Pinus sylvestris* (Jankowiak & Rossa 2007; Jankowiak 2010). The fungus has a frequently-observed asexual stage (Jacobs & Wingfield 2001), and is assumed to have a sexual stage based on the presence of mating type genes (Duong *et al.* 2013). Based on a recent study by Duong *et al.* (2013), *L. procerum* is a heterothallic fungus, meaning that each fungal culture possesses the genes for only one mating type, and must interact with individuals possessing the other mating type for meiosis to occur.

Leptographium procerum is frequently associated with the red turpentine beetle (*Dendroctonus valens*) in parts of the native range of the bark beetle in eastern North America (Taerum *et al.* 2013). The fungus appears to be a commensalist of the beetle, as the presence of *L. procerum* does not impact the development of *D. valens* larvae (Wang *et al.* 2012). Both the beetle and fungus are considered to be minor nuisances in North America, as the beetle primarily colonizes stressed or dying trees (Owen *et al.* 2010), while most pathogenicity trials have demonstrated that *L. procerum* gives rise to only small lesions on trees (Harrington 1988; Wingfield *et al.* 1988; Jankowiak *et al.* 2007; however, see Alexander *et al.* 1988).

Both *D. valens* and *L. procerum* appear to be more aggressive in their ranges in China. The beetle was accidentally introduced to China in the 1980's (Yan *et al.* 2005). *Leptographium procerum* was previously believed to have coinvaded China with *D. valens*, based on the fact that the fungus is associated with the beetle in its native range in eastern North America (Taerum *et al.* 2013), and that it has been reported in China as a symbiont of only this beetle (Lu *et al.* 2009a,b). Since 1999, *D. valens* has killed millions of healthy native pine trees in central China (Yan *et al.* 2005). Interactions between *D. valens* and *L. procerum* have been suggested to contribute to the tree-killing behaviour of the beetle as some *L. procerum* strains appear to be pathogenic to pines in China (Lu *et al.* 2010, 2011). In addition, there is evidence that trees infected with pathogenic strains of *L. procerum* in China may produce significantly larger quantities of the monoterpene 3-carene relative to healthy trees (Lu *et al.* 2010, 2011). This monoterpene is highly attractive to *D. valens*, and has been hypothesized to contribute to the tree-killing behaviour of the insect in China (Sun *et al.* 2013). This increased pathogenicity in China along with the production of more 3-carene could be due to rapid evolution of the fungus (Lu *et al.* 2011), although it could also be due to plasticity in the fungus or interactions with more susceptible hosts in China (Gladieux *et al.* 2014). Because *L. procerum* is the most common associate of *D. valens* in China (Lu *et al.* 2009a,b), it has been suggested that the fungus had a substantial impact on the outbreak dynamics of the bark beetle.

Although *L. procerum* has only been implicated as invasive in China (Lu *et al.* 2011; Sun *et al.* 2013; Taerum *et al.* 2013), it is present in many other locations around the world (Jacobs & Wingfield 2001). *Leptographium procerum* was originally described in eastern North America as an associate of several bark beetles and weevils (Kendrick 1962), and thus believed to be native to that continent. Later, the fungus was reported as an associate of various bark beetle and weevil species in England (Wingfield & Gibbs 1991), France (Piou 1993), Italy, Norway, the former Yugoslavia (Jacobs & Wingfield 2001), Poland (Jankowiak & Bilański 2013a,b,c), Russia (Linnakoski *et al.* 2012), Japan (Masuya *et al.* 2013), and New Zealand (Reay *et al.* 2005). Most of the studies in Europe and the study in Japan

Please cite this article in press as: Taerum SJ, et al., Putative origins of the fungus *Leptographium procerum*, Fungal Biology (2016), http://dx.doi.org/10.1016/j.funbio.2016.09.007

identified *L. procerum* strains based on morphology or the internal transcribed spacer 2 and partial large subunit (ITS2-LSU) of the ribosomal DNA region, neither of which vary among most species in the *L. procerum* species complex (Yin *et al.* 2015). However, three recent studies in Poland utilised part on the beta-tubulin (βT) gene region (Jankowiak & Bilański 2013a,b,c), which is adequately informative to differentiate *L. procerum* from the other fungi in the species complex (Yin *et al.* 2015). In addition, the single isolate reported from Russia was confirmed to be *L. procerum* based on multi-gene phylogenies (Yin *et al.* 2015). The *L. procerum* strains in Europe may be invasive (Linnakoski *et al.* 2012; Duong *et al.* 2013), although the fungus has been reported from several locations across the continent as an associate of numerous bark beetle and weevil species, suggesting that it might in fact be native in that region.

In this study we used microsatellites and mating type loci to examine the global diversity of a large collection of *L. procerum* isolates. We set out to address the following questions: 1) Where is the most probable centre of diversity of *L. procerum*; and 2) Did *L. procerum* coinvade China with *D. valens*?

Materials and methods

Collections and identification

Putative *Leptographium procerum* strains were obtained from the CMW Culture Collection of the Forestry and Agricultural Biotechnology Institute at the University of Pretoria, South Africa. These isolates had been earlier obtained from numerous locations including North America (Canada, USA; Fig 1), Europe (Czech Republic, England, France, Italy, Norway, Poland, Russia, the former Yugoslavia), and China. Because *L. procerum* is a non-obligate, externally-vectored fungus that varies in abundance over space and time, collections varied considerably between sampling locations. Often only small numbers of isolates could be collected from a location. All of the cultures from China were isolated from *Dendroctonus valens*. The collection details (i.e., sampling locations, insect vectors, tree hosts, and isolation methods) for each strain are summarized in Table S1.

Initial identifications were based on culture morphology. To confirm that the cultures represented *L. procerum*, part of the beta-tubulin (βT) gene region was sequenced. DNA was extracted using the technique described by Möller *et al.* (1992). DNA fragment amplification and sequencing were performed as described by Duong *et al.* (2012), using the primers Bt2a and Bt2b (Glass & Donaldson 1995). Sequences of each βT haplotype were aligned with three sequences for *L. procerum* in GenBank (see Fig S1 for accession numbers), as well as one sequence each for all other known species in the *L. procerum* species complex (Yin *et al.* 2015) and sequences for *Grosmannia alacris* and *Grosmannia serpens* (Duong *et al.* 2012) that were included as an outgroup, using the ClustalW method (Larkin *et al.* 2007) in MEGA 5 (Tamura *et al.* 2011). Maximum likelihood (ML) analyses were conducted in MEGA, and bootstrap support for the phylogenetic clades was calculated using 1000 ML replicates. Isolates that clustered with the reference *L. procerum* strains were used in subsequent analyses.

Microsatellites

To generate microsatellite markers, the genome of an isolate of *Leptographium procerum* (van der Nest *et al.* 2014) was mined for microsatellite sequences and primer pairs were developed to amplify the markers using MSATCOMMANDER 0.8.2

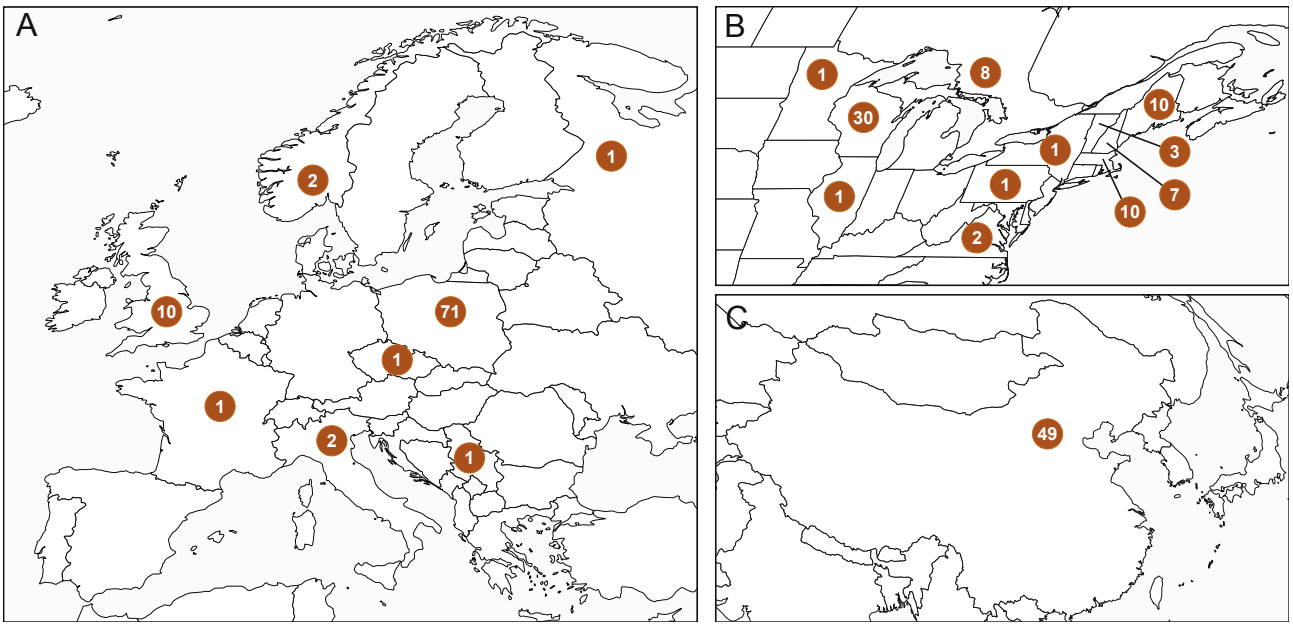

Fig 1 – Maps showing sampling locations of *L. procerum* isolates. Orange circles indicate that *L. procerum* was obtained from within the country, state, or province boundaries, while the numbers within the circles indicate the number of isolates collected from the area. (A) Collections in Europe; (B) collections in North America; (C) collections in China (For interpretation of the references to colour in this figure legend, the reader is referred to the web version of this article.).

Please cite this article in press as: Taerum SJ, et al., Putative origins of the fungus *Leptographium procerum*, Fungal Biology (2016), http://dx.doi.org/10.1016/j.funbio.2016.09.007

(Faircloth 2008). Thirty three microsatellite loci with repeat motifs ranging from three to six bases were selected for screening. Amplifications were conducted on three *L. procerum* isolates from the USA (CMW30664, CMW34542, CMW41210), three from Poland (CMW40806, CMW40807, CMW40809), and one from China (CMW 25648). PCRs were conducted in 12 μL mixtures containing 1 μL template DNA (10–50 ng), 8.4 μL dH_2O, 2 μL 5× MyTaq reaction buffer (Bioline, London, UK), 0.25 μL of each primer (10 μM), and 0.1 μL MyTaq (Bioline). PCR conditions were as follows: 96 °C for 2 min, followed by 30 cycles of 94 °C for 30 s, 58 °C for 30 s, and 72 °C for 60 s, followed by a final extension step of 72 °C for 45 min. Sequencing was conducted following Yin *et al.* (2015).

Fifteen polymorphic loci were selected for the genotyping of all *L. procerum* isolates that were obtained in this study (Table S2). Optimal multiplex reactions were determined using Multiplex Manager 1.0 (Holleley & Geerts 2009). Amplifications were then conducted using labelled primers following the above PCR protocol. Scoring by size was conducted using GeneMarker 2.2.0 (SoftGenetics, State College, PA, USA). All fungal isolates that showed double peaks when scored were assumed to represent mixed cultures, and were excluded from the study. After genotyping was completed, between 1 and 11 representatives per allele were amplified and sequenced using unlabelled primers. The global F_{ST} as well as F_{ST} values for each locus were calculated using the diveRsity package implemented in R (Keenan *et al.* 2013).

Network and clustering analyses

We first conducted network and clustering analyses to determine if isolates obtained from different geographical locations formed genetically distinct groups. The median-joining network among haplotypes was generated using Network 4.6.1.1 (http://www.fluxus-engineering.com). The maximum parsimony calculation option was used to determine the optimal network.

Clustering analyses were first conducted using the software STRUCTURE 2.3 (Pritchard *et al.* 2000). STRUCTURE uses Bayesian methods to divide a population data set into a prespecified number of genetic clusters that are in Hardy–Weinberg and linkage equilibrium, while simultaneously assigning individuals within the data set to each cluster. The software then calculates likelihood values for each K-value (i.e., number of genetic clusters to which individuals in the data set could be assigned) tested. Analyses were conducted using an admixture model of ancestry and a correlated allele frequencies model. For each run, one million Markov Chain Monte Carlo (MCMC) replicates were retained after a burn-in of 100 000. We conducted 20 runs for each K-value between 1 and 8. STRUCTURE runs with similar membership coefficients were grouped and averaged using CLUMPAK (Kopelman *et al.* 2015) for each K-value based on the Markov clustering algorithm (MCL). The cut-off MCL value was 0.9. In instances where there was multimodality (i.e., there was support for more than one pattern at a K-value), 100 STRUCTURE runs were conducted for those K-values following the above protocol. Bar charts showing mean membership coefficients were generated using CLUMPAK. The optimal K-value was determined following the Evanno method (Evanno *et al.* 2005) implemented with CLUMPAK. Mean membership coefficients for each individual were recorded at the selected K-values.

We also conducted clustering analysis with DAPC using the adegenet package (Jombart 2008) implemented in R. This method combines principal component analyses (PCA) and discriminant analyses (DA) to divide a data set into different genetic clusters so that the variance among clusters is maximized and the variance within clusters is minimized. PCA were conducted to simplify the data set, after which the Bayesian Information Criterion (BIC) was used to determine the most likely range of K-values. Following the recommendation of the creator of the adegenet package (Jombart 2014), an α-plot was generated to determine the optimal number of principal components to retain. DAPC was then conducted to assign the *Leptographium procerum* isolates to the different genetic clusters. After determining the most biologically meaningful K-values, DISTRUCT 1.1 (Rosenberg 2004) was used to create bar charts to visualize the membership probabilities. Membership probabilities for each individual were recorded at the selected K-values.

Genetic diversity and linkage disequilibrium

The mean number of distinct alleles and private alleles in each geographical region (based on clustering analyses: China, Europe, and North America; see Results) were calculated after rarefaction using ADZE 1.0 (Szpiech *et al.* 2008) because the regions contained different numbers of individuals. The numbers of MLG in each cluster were calculated using the poppr 2.01 package (Kamvar *et al.* 2014) implemented in R. Because of the variation in sample sizes in each region, estimated MLG values after rarefaction were also calculated using poppr. Basic diversity indices were calculated on the MLG within each region using poppr. Allele frequencies within each cluster were calculated using PopGene 1.31 (Yeh *et al.* 1997). Because the numbers of sampled species of insect vectors varied dramatically between the regions (see Results), we also conducted the above analyses using only *Leptographium procerum* genotypes isolated from the most common vectors in each region (*Dendroctonus valens* in China and North America, *Hylobius abietis* in Europe) to determine if observed differences in diversity were impacted by variation in the number of sampled species of insect associates.

MultiLocus 1.3 (Agapow & Burt 2001) was used to test for linkage disequilibrium among loci in the geographically-distinct *L. procerum* populations. This was done because linkage disequilibrium could indicate if *L. procerum* from the geographical regions had recently undergone a genetic bottleneck as frequently occurs during introduction events. After the data set was clone-corrected, indices of association (I_A) and $\bar{r}_d$ values were calculated and compared with 1000 randomized data sets to determine whether any populations differed significantly from a population that is in linkage equilibrium.

Differentiation

Analysis of molecular variance (AMOVA) was conducted using GenAlEx 6.5 (Peakall & Smouse 2012) to partition the variance among and within the three geographical regions. In addition, pairwise comparisons were conducted between each region

Please cite this article in press as: Taerum SJ, et al., Putative origins of the fungus *Leptographium procerum*, Fungal Biology (2016), http://dx.doi.org/10.1016/j.funbio.2016.09.007

using AMOVA to test for panmixis between any of the geographical regions. In each analysis, 999 permutations were used.

Global migration of Leptographium procerum

We used Approximate Bayesian Computation (ABC; Beaumont *et al.* 2002) to discern among different evolutionary and demographic models, or 'scenarios,' that may explain the contemporary distribution and genetic diversity of *L. procerum*. ABC analyses were conducted using the coalescent-based software DIYABC 2.0.4 (Cornuet *et al.* 2014). This software allows the comparison of multiple scenarios, which are represented by coalescent trees that have different topologies. DIYABC simulates data sets for each scenario, and then compares selected summary statistics of the simulated data sets and the observed data set to determine posterior probabilities for each scenario. The scenario with the highest probability can then be selected as the 'best' scenario. The software also estimates model parameters such as effective population size, timing of past events (measured in generations), and mutation rates of molecular markers.

The geographical regions (China, Europe, and North America) were treated as populations in DIYABC in these analyses. Analyses were conducted using a clone-corrected data set to ensure that the presence of clonal replicates did not bias the estimates of effective population sizes. The categories of summary statistics compared were NAL, HET, VAR, MGW, N2P, H2P, V2P, and FST (see DIYABC user manual for descriptions of each statistic). Mutation rates of microsatellites with different lengths of repeat motifs (three, four, and six nucleotides) were calculated separately.

We used a stepwise approach to determine the most likely scenario. In step 1 of our analyses, we assumed that the populations arose from an ancestral population at the same time (i.e., as a polytomy). We then compared eight scenarios (summarized in Table S3) where zero or more clusters underwent a genetic bottleneck. Tests for bottlenecks were conducted first because it was assumed that introduced populations would show a signal of a bottleneck, while native populations would not. The topology (i.e., the relationship among the populations) was then tested in the following step. The prior ranges for the effective population sizes for each geographical population were initially set between 10 and 100 000, and the mutation rates for the microsatellites were set to the default ranges. Based on the posterior distributions of the initial analyses, later analyses were conducted with more restricted prior ranges so that the effective population sizes of each cluster and the mutation rates of the microsatellite loci could be more accurately estimated (summarized in Table S4). One million data sets were simulated for each scenario. Posterior probabilities of each scenario were calculated from the Euclidean distance between the summary statistics of the observed and simulated data sets based on multinomial logistic regression.

In step 2, four scenarios (Table S3) were compared based on the outcome of step 1. Here, we relaxed the assumption that the clusters diverged at the same time and allowed the clusters that underwent genetic bottlenecks based on step 1 to diverge from the other clusters at different time points (prior ranges are summarized in Table S4). The ranges for effective population sizes and mutation models were based on the results of step 1. After determining the best scenario in step 2, the median, mode, mean, and 95 % confidence intervals of the estimated parameters were recorded. The model checking option in DIYABC was performed to test for goodness of fit of the model to the data. The categories of summary statistics used for model checking were LIK, DAS, and DM2 (refer to DIYABC manual for details on each statistics). In total, 36 summary statistics that had not been used in the previous analyses were used for model checking.

To assess if the power of the analyses was sufficient to discriminate between the different scenarios, type I and II errors were calculated for the best scenarios in steps 1 and 2. One hundred data sets were generated for each scenario using the same prior distributions as the previous analyses. Posterior probabilities of each scenario were then calculated for each simulated data set. Type I error was calculated by measuring the proportion of times the best scenario did not have the highest posterior probability when it was in fact the correct scenario. Type II error was calculated by measuring the proportion of times the best scenario had the highest posterior probability when it was not the correct scenario.

Mating type loci

The ratios between mating type genes *MAT1-1-3* and *MAT1-2-1* (herein referred to as MAT1 and MAT2 respectively) in each geographical location were determined using the technique described by Duong *et al.* (2013). Chi-square tests were used to test for significant differences between the observed ratios between MAT1 and MAT2 and the 1:1 ratio expected in a randomly-mating population. Isolates that had both mating types most likely represented mixed cultures, and were excluded from the calculations of mating type ratios.

Results

Collections

In total, 211 confirmed *Leptographium procerum* strains were obtained: 49 from China, 73 from North America, and 89 from Europe (Fig 1, Table S1). All of the isolates retained in the study had identical βT sequences and grouped with the *L. procerum* sequences downloaded from GenBank in phylogenetic analyses (Fig S1).

Microsatellites

Fifteen of the 33 tested microsatellite loci were polymorphic (GenBank accession numbers KU365065–KU365079). The summary statistics of the microsatellite loci are summarized in Table S2. One allele of Lp20 that was 294 bases long had an 18 base deletion in the flanking region (Appendix S1). This allele was impossible to distinguish from another 294 base allele based on Genescan because the microsatellite repeat motif for this locus was six bases in length. However, alleles of 294 bases were found only four times in the entire data set. Likewise, the deletion in the flanking region was not

Please cite this article in press as: Taerum SJ, et al., Putative origins of the fungus *Leptographium procerum*, Fungal Biology (2016), http://dx.doi.org/10.1016/j.funbio.2016.09.007

observed in any other sequence of locus Lp20, and we could assume that the deletion had occurred only once in the entire data set. In addition, one allele of Lp31 (181 bases) had a 2 base deletion in the flanking region. These alleles were included in the subsequent analyses. All other loci varied in length only because of differences in the number of microsatellite repeats.

Network and clustering analyses

In the median-joining network, the nine haplotypes from China all occurred on one distinct branch separated from the other haplotypes (Fig 2). The Chinese haplotypes were most similar to some of the European haplotypes, as there was only one node separating the closest Chinese and European haplotypes. However, there were only three nodes separating the closest Chinese and North American haplotypes. The remainder of the network consisted of haplotypes from Europe and North America. Some of the haplotypes from Europe and North America were intermixed, although the majority of haplotypes clustered with other haplotypes from the same geographical origin. There was no evidence of geographical structure in haplotypes within Europe or North America, nor was there evidence of genetic structure within either continent based on insect vector or tree host, where such data were available.

For the STRUCTURE analyses, the Evanno method (Evanno *et al.* 2005) supported K = 3 as the optimal number of clusters in which to divide the data set as ΔK was highest at that K-value (Fig S2). However, we also analysed the data sets at K = 2 (to determine if the analyses at K = 2 gave any information regarding the relationship between the inferred clusters at K = 3) and K = 4 (because the ΔK was relatively high at K = 4). There was multimodality at K = 2 as two patterns were supported: 62 of 100 runs at K = 2 supported a pattern where the individuals from North America and Europe formed one cluster separate from the individuals from China (Fig 3), while 36 runs supported a pattern where the individuals from North America and China formed one cluster separate from the individuals from Europe. At K = 3, the data set was divided into three separate clusters: a yellow cluster that contained the isolates from China, a purple cluster that contained most of the isolates from North America and some from Europe, and a blue cluster that contained most of the individuals from Europe and some from North America. At K ≥4, STRUCTURE did not further subdivide the clusters based on geography, tree host, or insect vector.

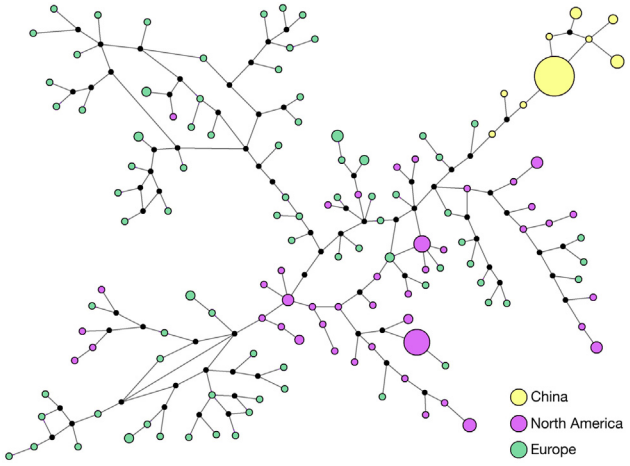

Fig 2 – Median-joining network showing the interrelationship among the *L. procerum* haplotypes. Circle diameter increases with more clones per haplotype. Smaller black dots represent median vectors, or hypothesized ancestors.

For the DAPC analyses, five was selected as the optimal number of principal components retained based on the α-plot (Fig S3a). The optimal K-value was not clear based on the plot of K-values and BIC (Fig S3b), although reductions in BIC appeared to be negligible with K-values larger than 8. We therefore selected K-values based on biological relevance. K-values between 2 and 4 were selected for analyses to compare with the STRUCTURE results. At K = 2, DAPC placed the isolates from China in one cluster and the isolates from North America and Europe in another cluster (Fig 3). At K = 3, the isolates from China were placed in one cluster, most isolates from North America and some from Europe were placed in a second cluster, and most isolates from Europe and some from North America were place in a third cluster. At K = 4, some individuals from Europe and North America were placed in a fourth cluster (shown in orange), although this subdivision was not informative based on geography, host or vector.

Based on the consensus of both clustering methods, K = 3 was the optimal number of clusters in which to divide the data set. Forty seven individuals (95.9 % of total individuals; Table S5) from China were clearly assigned (i.e., membership coefficient or membership probability >0.8) to the yellow cluster based on STRUCTURE. All 49 individuals from China were clearly assigned to the yellow cluster based on DAPC. STRUCTURE clearly assigned sixty seven individuals from North America (91.8 %) and two from Europe (2.2 %) to the purple cluster. DAPC clearly assigned seventy individuals from North America (95.9 %) and 28 individuals from Europe (31.5 %) to the purple cluster. STRUCTURE clearly assigned eighty individuals from Europe (89.8 %) and five individuals from North America (6.8 %) to the blue cluster. DAPC clearly assigned 55 individuals from Europe (61.8 %) and three individuals from North America (4.1 %) to the blue cluster.

Genetic diversity and linkage disequilibrium

There were nine haplotypes in the Chinese isolates, 42 in the North American isolates, and 81 in the European isolates. The numbers of isolates per haplotype ranged from one to 29 (Table S1). The ratios of haplotypes to isolates (measured by numbers of haplotypes divided by numbers of isolates examined) were 0.91 for Europe, 0.58 for North America, and 0.18 for China.

The isolates from Europe were the most genetically diverse based on mean numbers of alleles and private alleles which were calculated after rarefaction because the different geographical regions contained different numbers of individuals (Table 1). In addition, Europe had the highest genetic diversity based on estimated multilocus genotypes (MLG) calculated after rarefaction, as well as various diversity indices calculated on the MLG. This was also true when only comparing *Leptographium procerum* isolated from the most collected insect species in each location (Table S6). North America had the next

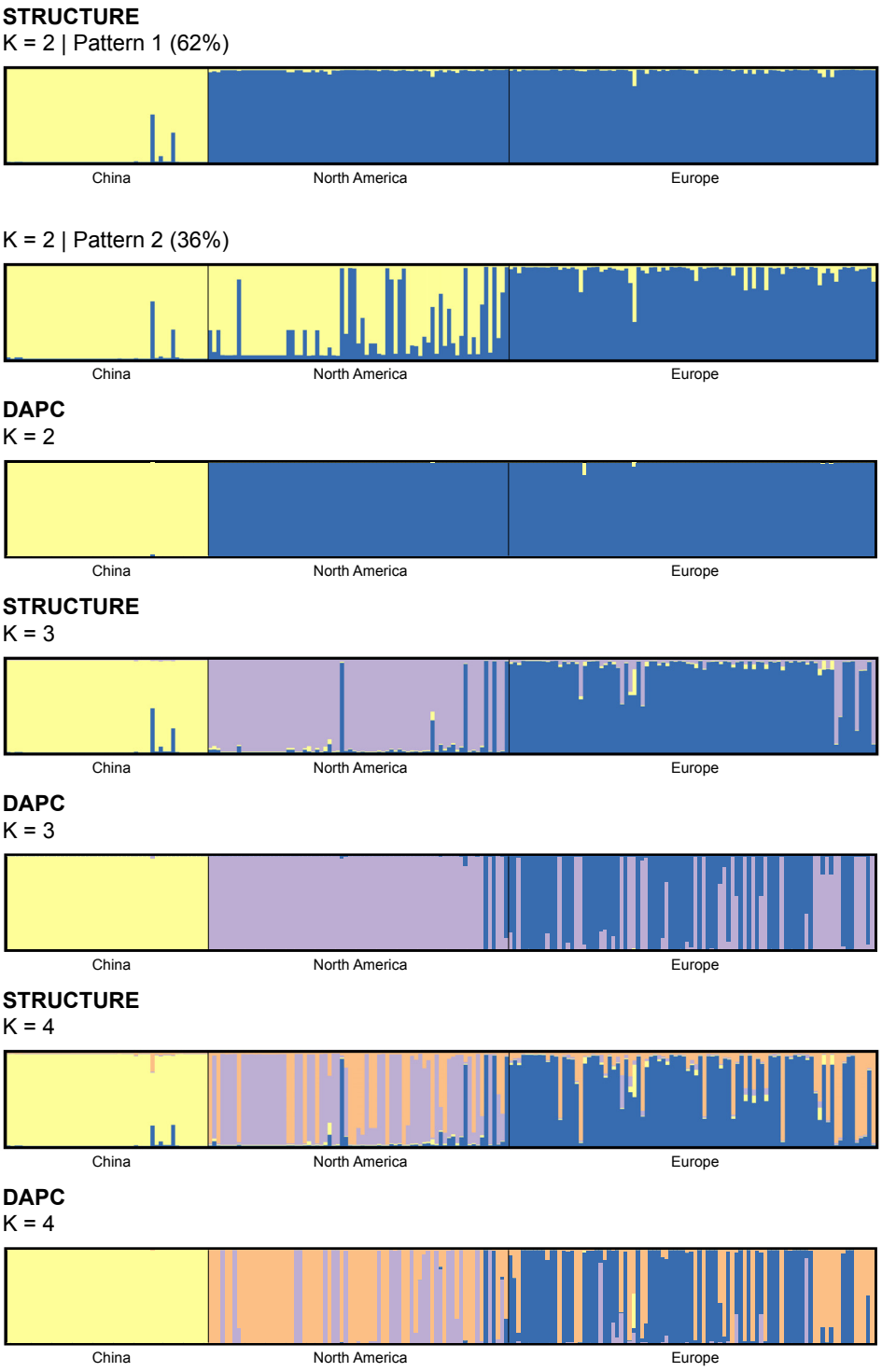

Fig 3 – Bar charts showing the membership coefficients (based on STRUCTURE) and the membership probabilities (based on DAPC) of the individuals included in this study for K-values between 2 and 4.

highest genetic diversity, followed by China. There were seven monomorphic loci in the Chinese isolates, one in the North American isolates, and none in the European isolates. The allele frequencies for each population are summarized in Table S7. Ninety two percent of the alleles found in China were present in Europe. In contrast, 67 % of the alleles found in China were present in North America. Seventy three percent of the alleles found in North America were also present in Europe, while 40 % of the alleles found in Europe were also present in North America.

There was no evidence of linkage disequilibrium in the Chinese or European collections based on IA and $\bar{r}_d$ values ($P = 0.201$ and 0.139, respectively; Table 2; Fig S4). However, there was strong evidence for linkage disequilibrium in the

Please cite this article in press as: Taerum SJ, et al., Putative origins of the fungus *Leptographium procerum*, Fungal Biology (2016), http://dx.doi.org/10.1016/j.funbio.2016.09.007

Table 1 – Summary statistics for the three genetic clusters of *L. procerum* examined in this study.

Cluster	MA	s.e.	PA	s.e.	eMLG	s.e.	ML	H	G	λ	He
China	1.600	0.163	0.196	0.133	9	0	7	1.14	1.91	0.476	0.262
North America	3.243	0.323	1.030	0.252	31.2	1.96	1	3.34	15.36	0.935	0.478
Europe	5.163	0.549	2.609	0.520	46.5	1.26	0	4.36	74.03	0.986	0.634

MA – mean allelic richness (after rarefaction); s.e. – standard error; PA – private allelic richness (after rarefaction); eMLG – estimated number of multilocus genotypes (after rarefaction); ML – monomorphic loci; H – Shannon–Wiener Index of MLG; G – Stoddart and Taylor's Index of MLG; λ – Simpson's index; He – expected heterozygosity (Nei 1973).

Table 2 – Linkage disequilibrium and mating type statistics for the four populations examined in this study.

	I_A	$\bar{r}_d$	P-value	MAT1:MAT2	X^2 P-value
China	0.2214	0.0319	0.201	45:4	<0.001
North America	0.5463	0.0440	<0.001	40:33	0.413
Europe	0.0728	0.0051	0.139	47:40	0.453

I_A – Index of Association; P-value for I_A and $\bar{r}_d$ are equal.

North American collections, as the observed IA and $\bar{r}_d$ values fell outside the range of most of the 1000 randomized data sets ($P < 0.001$).

Differentiation

The AMOVA indicated that most of the variation (75 %) was within populations (Table 3). However, there was significant among population variation (25 %). In addition, there was significant variation among the populations in the pairwise AMOVAs, rejecting the hypothesis of panmixis between any of the populations.

Global migration of Leptographium procerum

Scenario 5 (i.e., the clusters in North America and China had undergone a genetic bottleneck, while the cluster in Europe had not; Fig S5), had the highest probability ($P = 0.5895$, 95 % C.I. = 0.5198 to 0.6593; Table S3). Scenario 8 (i.e., all three clusters arose from an unsampled, or 'ghost,' population and had undergone genetic bottlenecks) also had high support ($P = 0.3912$, 95 % C.I. = 0.2894–0.4930).

In step 2, four scenarios (Table S3) were compared based on the outcome of step 1. Here, we relaxed the assumption that the clusters diverged at the same time and allowed the clusters that underwent genetic bottlenecks based on step 1 (North America and China) to diverge from the other clusters at different time points. Scenario 5.1, (i.e., both the Chinese and North American clusters diverged from the European cluster, with the Chinese cluster arising earlier than the North American cluster; Fig S5), had the highest probability ($P = 0.5948$, 95 % C.I. = 0.4821–0.7075). There was non-trivial support for hypothesis 5.3 (i.e., the North American cluster first diverged from the European cluster, after which the Chinese cluster diverged from the North American cluster; $P = 0.2613$, 95 % C.I. = 0.0753–0.4473).

The estimates of the model parameters for scenario 5.1 are summarized in Table S4. The modes, medians, and means of

Table 3 – AMOVA results for the complete data set as well as pairwise comparisons.

Source	Degrees of freedom	Sum of squares	Mean squares	Estimated variance	% Total variance
All three geographical populations					
Among populations	2	21 476.966	10 738.483	150.355	25
Within populations	208	94 083.773	452.326	452.326	75
Total	210	115 560.739		602.681	100
$\varphi PT = 0.249$	$P < 0.001$				
North America and Europe					
Among populations	1	7518.462	7518.462	86.473	13
Within populations	160	93 197.365	582.484	582.484	87
Total	161	100 715.827		668.956	100
$\varphi PT = 0.129$	$P < 0.001$				
China and North America					
Among populations	1	14 365.373	14 365.373	238.966	40
Within populations	120	42 304.627	352.539	352.539	60
Total	121	56 670.000		591.505	100
$\varphi PT = 0.404$	$P < 0.001$				
China and Europe					
Among populations	1	11 307.837	11 307.837	172.786	31
Within populations	136	52 665.554	387.247	387.247	69
Total	137	63 973.391		560.033	100
$\varphi PT = 0.309$	$P < 0.001$				

Please cite this article in press as: Taerum SJ, et al., Putative origins of the fungus *Leptographium procerum*, Fungal Biology (2016), http://dx.doi.org/10.1016/j.funbio.2016.09.007

the posterior distributions of each parameter were fairly similar. The European population had the highest effective population size, followed by the North American and Chinese clusters respectively. Based on the goodness of fit test for scenario 5.1, only four summary statistics (out of 36) had low probability values (Table S8). The type I error for scenario 5 was 0.46 suggesting that there was a high probability of selecting an incorrect scenario when simulating data sets for scenario 5. Thirty two of the incorrectly assigned pseudodata were assigned to scenario 8, while ten were assigned to scenario 2. The type II error for scenario 5 was 0.04. The type I error for scenario 5.1 was 0.14, while the type II error was 0.09.

Mating types

There was no significant bias towards either mating type in the European or North American populations. Conversely, there was a significant bias towards mating type MAT1 for isolates from China (Table 2; Fig S6).

Discussion

Results of this study demonstrated that Europe or a location geographically and genetically close to Europe is the likely global centre of diversity of *Leptographium procerum*. In contrast, populations of the fungus in North America and China appear to have been founded by introduced isolates. In addition, clustering and network analyses along with ABC suggested that Europe (or its vicinity) is the most probable source of *L. procerum* associated with *Dendroctonus valens* in China. This finding does not support the hypothesis that *L. procerum* coinvaded China from North America with *D. valens* (Lu *et al.* 2011; Sun *et al.* 2013; Taerum *et al.* 2013).

The conclusion that Europe is the global centre of diversity of *L. procerum* emerged from four lines of evidence: 1) the lack of bias towards either of the two mating types in Europe; 2) a failure to demonstrate a departure from linkage equilibrium in Europe; 3) the fact that the isolates from that geographical region had the highest level of genetic diversity of all the isolates included in this study; and 4) the results of the ABC analyses showing that Europe is the most likely source of the other populations examined. The observations regarding mating type ratio and linkage equilibrium suggest that the fungus is randomly mating in Europe. In addition, the observed high level of genetic diversity and large number of rare alleles in the European population are frequently characteristics of old and stable (i.e., native) populations (Sakai *et al.* 2001; Zhang *et al.* 2014). The high diversity of *L. procerum* in Europe combined with the close proximity of Europe to Asia, which appears to be the centre of diversity for species in the *L. procerum* species complex (Linnakoski *et al.* 2012; Yin *et al.* 2015), support the suggestions that Europe or somewhere close to Europe is the global centre of diversity of *L. procerum*.

Three differences in sampling schemes between the locations may have impacted the observed variation in genetic diversity: 1) the highest number of isolates was collected in Europe, followed by North America and China; 2) *L. procerum* was isolated from a wider diversity of insect vectors in Europe than in North America and China; and 3) *L. procerum* was isolated from a broader geographical range in Europe (the furthest apart sampling locations, Herouville St. Clair, France, and Lissino-Corpus, Russia, were separated by ~2250 km) than North America (Zimmerman, Minnesota, and the Massabesic Experimental Forest, Maine were separated by ~1650 km) or China (collection sites were separated by <1000 km). However, the genetic diversity in Europe remained the highest after applying a rarefaction method, negating the impact of differences in sample sizes on diversity indices. In addition, diversity measurements of *L. procerum* isolated from only a single insect species in each location (*Hylobius abietis* in Europe and *D. valens* in North America and China) still supported Europe as having the highest genetic diversity. These results were obtained even though fewer isolates were considered for Europe (N = 38) compared with North America (N = 60) and China (N = 49). In this case, all of the *L. procerum* isolates from Europe were collected in Poland, while the North American isolates were from a much larger geographical range, suggesting that differences in sampling ranges did not greatly impact the observed pattern of diversity.

It is noteworthy that the majority of *L. procerum* isolates that were obtained from Europe (71 out of 89) were collected in Poland. The apparent bias towards Poland is largely because *L. procerum* is frequently associated with *Pinus sylvestris*, which is the dominant tree species in Poland (Jankowiak 2006, 2012; Jankowiak & Bilanski 2013a,b,c; Jankowiak *et al.* 2007, 2012). In the Polish lowlands, the proportion of *P. sylvestris* in the forests is about 70 % (Boratyński 1993). Therefore, although Poland is not likely to be entirely representative of the continent, the country is most likely a major centre of diversity.

The fungus *L. procerum* was until now considered to be native to North America, but our study provides evidence that the North American population of *L. procerum* may have recently originated in Europe, after which the fungus developed an association with *D. valens* and other beetles in eastern North America. The haplotypes from both locations grouped together in the clustering and network analyses, and the European cluster had higher genetic diversity than the North American cluster. In addition, there was strong evidence of linkage disequilibrium in the North American cluster but not in the European cluster. Finally, ABC supported the hypothesis that Europe is the origin of the North American cluster. The introduction of *L. procerum* into North America could have occurred via the movement of wood or wood products from Europe. Because the fungus in eastern North America is fairly genetically diverse and widespread, and there is no bias toward either mating type, the introductions would need to have been large or frequent, and to have occurred far enough in the past to allow the fungus to spread to its current range. Considering that *L. procerum* requires insect vectors to disperse, and that most of the vectors of *L. procerum* that occur at both locations were introduced to one of the continents within the past century, it is unlikely that the fungus would have been moved from one continent to the other without the assistance of humans. Additional collections of *L. procerum* isolates from Europe and North America as well as coalescent analyses would be required to test these hypotheses.

This study supports the hypothesis that the isolates of *L. procerum* in China underwent a strong founding event. The low diversity of the fungus in China relative to the populations

Please cite this article in press as: Taerum SJ, et al., Putative origins of the fungus *Leptographium procerum*, Fungal Biology (2016), http://dx.doi.org/10.1016/j.funbio.2016.09.007

in Europe and North America can suggest a recent genetic bottleneck. In addition, the bias towards mating type MAT1 in the Chinese population is consistent with a shift to clonal reproduction that frequently occurs in fungi alongside genetic bottlenecks (Gladieux *et al.* 2014). The cause of the bottleneck, however, is unknown. The fungus may have been recently introduced by humans, as there has been a long history of movement of people and goods between Europe and Asia. Alternatively, the fungus may have undergone a recent natural range expansion, whereby *L. procerum* could have colonized China from Europe via the conifer forest 'bridges' connecting the two geographical regions by bark beetle species that presently occur in both locations (e.g., *Tomicus piniperda*, *Tomicus minor*; Kirisits 2004; Zhou *et al.* 2013). According to this hypothesis, the low diversity of the fungus in China would indicate the range edge for *L. procerum*, as those areas tend to have lower genetic diversities than range interiors (Arnaud-Haond *et al.* 2006). A third alternative hypothesis is that *L. procerum* was introduced to China much further in the past, and is associated with other beetle species that occur in China. Most surveys of ophiostomatalean fungi in China have been conducted on associates of damaging bark beetle species, while relatively benign bark beetles and weevils have been largely ignored (Zhou *et al.* 2013). It is possible that only a small number of *L. procerum* haplotypes was acquired from these native beetles by introduced *D. valens*, after which point these haplotypes benefitted from the beetle's population explosion, with clones of this fungus propagating more rapidly than other haplotypes of *L. procerum* present in the invasive range of *D. valens* in China.

Based on previous surveys of the ophiostomatalean fungi associated with *D. valens* in China and North America, *L. procerum* is the only fungal species that was an abundant symbiont of *D. valens* in both China (Lu *et al.* 2009a,b) and part of the beetle's range in North America (eastern North America; Taerum *et al.* 2013). This led researchers to conclude that *L. procerum* is the only fungus likely to have coinvaded China with *D. valens*. However, population genetics studies on the beetle concluded that western North America is the most likely source of *D. valens* that invaded China (Cognato *et al.* 2005; Cai *et al.* 2008; Taerum *et al.* 2016). The fact that *L. procerum* is not associated with *D. valens* in western North America (Taerum *et al.* 2013) combined with the findings of the present study suggest that *L. procerum* did not coinvade China with the bark beetle. It is possible that none of the ophiostomatalean fungi symbiotic with *D. valens* in North America successfully coinvaded China with the bark beetle. The entire ophiostomatalean symbiont assemblage of *D. valens* in China appears to have been acquired from the invasive range, most likely from bark beetles and weevils that cooccur with *D. valens* in infested trees. However, it is not yet possible to definitively state that no isolates of *L. procerum* coinvaded China with *D. valens*.

A question however remains (Taerum *et al.* 2013): why have none of the ophiostomatalean symbionts of *D. valens* successfully coinvaded China? The relative high diversity of *D. valens* in China suggests that a large number of beetles were introduced either in a single mass invasion or multiple smaller invasions (Taerum *et al.* 2016), making it unlikely that no ophiostomatalean fungi would have survived the invasion event. Because the ophiostomatalean associates of *D. valens* are externally vectored and not protected by structures such as mycangia (Taerum *et al.* 2013), the fungi could have been susceptible to unfavourable environmental conditions. In addition, ophiostomatalean fungi already present in China could have outcompeted any North American fungi carried by the beetles to China. This could represent an example of biotic resistance by native microbes (Inderjit & van der Putten 2010). In addition, several interactions between forest insects and ophiostomatalean fungi are mediated by mites (Hofstetter & Moser 2014). Mite associates may have undergone a shift since the beetle was introduced, leading to a shift in the fungal symbionts. This finding is in contrast with surveys of yeast associates of *D. valens* in western North America and China, which demonstrated that several yeast species are likely to have coinvaded China with the beetle (Lou *et al.* 2014). Several of the coinvading yeasts were isolated from the beetle guts, which would have provided protection for the yeasts from unsuitable environmental conditions and antagonists of the yeasts.

This study represents the first global study of the population diversity of *L. procerum*, and the first attempt to determine the global movement of the fungus beyond its introduction to China (Lu *et al.* 2011). Our results do not support the hypothesis that *L. procerum* coinvaded China from North America with *D. valens*, and suggest that Europe is both the centre of global diversity and the source for all introduced populations. Future surveys should be conducted to test alternative hypotheses, including whether *L. procerum* is native or introduced in China. In addition, other genetic markers that are available due to advancements in high-throughput sequencing together with advanced analytical methods should clarify both the evolutionary history of *L. procerum* as well as the current global movement of the fungus. Nevertheless, this study has provided a basis for improving the understanding and management of *L. procerum*, as well as other invasive fungi.

Acknowledgements

We thank Carline Carvalho, Kevin Dodds, Nancy Gillette, Jianghua Sun, Lu Min, Ken Raffa and XuDong Zhou for invaluable assistance with collections of *L. procerum*. Funding was provided by the bilateral agreement between the Governments of South Africa and China, via project 2012DFG31830 (International Science & Technology Cooperation Program of China). In addition, financial support was provided by the Department of Science and Technology (DST)/National Research Foundation (NRF) Centre of Excellence in Tree Health Biotechnology. This project was supported by multiple grants from the NRF, South Africa, including the grant specific unique reference number (UID) 83924. The grant holders acknowledge that opinions, findings, and conclusions or recommendations expressed in publications generated by NRF supported research are that of the authors, and the NRF accepts no liability whatsoever in this regard.

Appendix A. Supplementary data

Supplementary data related to this article can be found at http://dx.doi.org/10.1016/j.funbio.2016.09.007.

REFERENCES

Agapow PM, Burt A, 2001. Indices of multilocus linkage disequilibrium. *Molecular Ecology Notes* **1**: 101–102.

Alexander SA, Horner WE, Lewis KJ, 1988. *Leptographium procerum* as a pathogen of pines. In: Harrington TC, Cobb Jr FW (eds), Leptographium *Root Diseases on Conifers*. APS Press, St. Paul, Minnesota, pp. 97–112.

Arnaud-Haond S, Teixeira S, Massa SI, Billot C, Saenger P, Coupland G, Duarte CM, Serrão EA, 2006. Genetic structure at range edge: low diversity and high inbreeding in Southeast Asian mangrove (*Avicennia marina*) populations. *Molecular Ecology* **15**: 3515–3525.

Beaumont MA, Zhang WY, Balding DJ, 2002. Approximate Bayesian computation in population genetics. *Genetics* **162**: 2025–2035.

Boratyński A, 1993. Systematics and geographical distribution. In: Białobok S, Boratyński A, Bugała W (eds), *Biology of Scots Pine*, p. 4570 Sorus, Poznań, Kórnik (in Polish).

Cai YW, Cheng XY, Xu RM, Duan DH, Kirkendall LR, 2008. Genetic diversity and biogeography of red turpentine beetle *Dendroctonus valens* in its native and invasive regions. *Insect Science* **15**: 291–301.

Cardoza YJ, Klepzig KD, Raffa KF, 2006. Bacteria in oral secretions of an endophytic insect inhibit antagonistic fungi. *Ecological Entomology* **31**: 636–645.

Cognato AI, Sun JH, Anducho-Reyes MA, Owen DR, 2005. Genetic variation and origin of red turpentine beetle (*Dendroctonus valens* LeConte) introduced to the People's Republic of China. *Agricultural and Forest Entomology* **7**: 87–94.

Cornuet J-M, Puldo P, Veyssier J, Dehne-Garcia A, Gautier M, Leblois R, Marin J-M, Estoup A, 2014. DIYABC v2.0: a software to make approximate Bayesian computation inferences about population history using single nucleotide polymorphism, DNA sequence and microsatellite data. *Bioinformatics* **30**: 1187–1189.

Duong TA, de Beer ZW, Wingfield BD, Wingfield MJ, 2012. Phylogeny and taxonomy of species in the *Grosmannia serpens* complex. *Mycologia* **104**: 715–732.

Duong TA, de Beer ZW, Wingfield BD, Wingfield MJ, 2013. Characterization of the mating-type genes in *Leptographium procerum* and *Leptographium profanum*. *Fungal Biology* **117**: 411–421.

Estoup A, Guillemaud T, 2010. Reconstructing routes of invasion using genetic data: why, how and so what? *Molecular Ecology* **19**: 4113–4130.

Evanno G, Regnaut S, Goudet J, 2005. Detecting the number of clusters of individuals using the software STRUCTURE: a simulation study. *Molecular Ecology* **14**: 2611–2620.

Faircloth BC, 2008. MSATCOMMANDER: detection of microsatellite repeat arrays and automated, locus-specific primer design. *Molecular Ecology Resources* **8**: 92–94.

Fisher MC, Garner TWJ, 2007. The relationship between the emergence of *Batrachochytrium dendrobatidis*, the international trade in amphibians and introduced amphibian species. *Fungal Biology Reviews* **21**: 2–9.

Gladieux P, Feurtey A, Hood ME, Snirc A, Clavel J, Dutech C, Roy M, Giraud T, 2014. The population biology of fungal invasions. *Molecular Ecology*. http://dx.doi.org/10.1111/mec.13028.

Glass NL, Donaldson GC, 1995. Development of primer sets designed for use with the PCR to amplify conserved genes from filamentous ascomycetes. *Applied and Environmental Microbiology* **61**: 1323–1330.

Harrington TC, 1988. *Leptographium* species, their distributions, hosts and insect vectors. In: Harrington TC, Cobb Jr FW (eds), Leptographium *Root Diseases on Conifers*. APS Press, St. Paul, Minnesota, pp. 1–40.

Hofstetter RW, Moser JC, 2014. The role of mites in insect-fungus associations. *Annual Review of Entomology* **59**: 537–557.

Holleley CE, Geerts PG, 2009. Multiplex Manager 1.0: a cross-platform computer program that plans and optimizes multiplex PCR. *Biotechniques* **46**: 511–517.

Hulcr J, Dunn RR, 2011. The sudden emergence of pathogenicity in insect–fungus symbioses threatens naive forest ecosystems. *Proceedings. Biological Sciences* **278**: 2866–2873.

Inderjit, van der Putten WH, 2010. Impacts of soil microbial communities on exotic plant invasions. *Trends in Ecology and Evolution* **25**: 512–519.

Jacobs K, Wingfield MJ, 2001. Leptographium *Species – tree pathogens, insect associates, and agents of blue-stain*. APS Press, St. Paul, Minnesota.

Jankowiak R, 2006. Fungi associated with *Tomicus piniperda* in Poland and assessment of their virulence using Scots pine seedlings. *Annals of Forest Science* **63**: 801–808.

Jankowiak R, Rossa R, 2007. Filamentous fungi associated with *Monochamus galloprovincialis* and *Acanthocinus aedilis* (Coleoptera: Cerambycidae) in Scots pine. *Polish Botanical Journal* **52**: 143–149.

Jankowiak R, Rossa R, Bilański P, 2007. Contribution to pathogenicity of three blue-stain fungi associated with the pine sawyer beetle (*Monochamus galloprovincialis*) (Coleoptera: Cerambycidae) to Scots pine in Poland. *Phytopatologia Polonica* **46**: 37–46.

Jankowiak R, 2010. Grzyby z grupy *Ophiostoma sensu lato* związane z kózkowatymi, *Monochamus sutor* (L.) i *Rhagium inquisitor* (L.) w południowej Polsce. *Sylwan* **154**: 381–387.

Jankowiak R, 2012. Ophiostomatoid fungi associated with *Ips sexdentatus* on *Pinus sylvestris* in Poland. *Dendrobiology* **68**: 43–53.

Jankowiak R, Bilański P, Kolařík M, Wasiuta D, 2012. Root-colonizing ophiostomatoid fungi associated with dying and dead young Scots pine in Poland. *Forest Pathology* **42**: 492–500.

Jankowiak R, Bilański P, 2013a. Association of the pine-infesting *Pissodes* species with ophiostomatoid fungi in Poland. *European Journal of Forest Research* **132**: 523–534.

Jankowiak R, Bilański P, 2013b. Ophiostomatoid fungi associated with root-feeding bark beetles on Scots pine in Poland. *Forest Pathology* **43**: 422–428.

Jankowiak R, Bilański P, 2013c. Diversity of ophiostomatoid fungi associated with the large pine weevil, *Hylobius abietis*, and infested Scots pine seedlings in Poland. *Annals of Forest Scienc* **70**: 391–402.

Jombart T, 2008. adegenet: a R package for the multivariate analysis of genetic markers. *Bioinformatics* **24**: 1403–1405.

Jombart T, 2014. *A Tutorial for Discriminant Analysis of Principal Components (DAPC) Using* adegenet 1.4–1. http://cran.r-project.org/web/packages/adegenet/.

Kamvar ZN, Tabima JF, Grünwald NJ, 2014. *Poppr*: an R package for genetic analysis of populations with clonal, partially clonal, and/or sexual reproduction. *PeerJ* **2**: e281.

Keenan K, McGinnity P, Cross TF, Crozier WW, Prodoehl PA, 2013. diveRsity: an R package for the estimation and exploration of population genetics parameters and their associated errors. *Methods in Ecology and Evolution* **4**: 782–788.

Kendrick WB, 1962. The *Leptographium* complex. *Verticicladiella* Hughes. *Canadian Journal of Botany* **40**: 771–797.

Kirisits T, 2004. Fungal associates of European bark beetles with special emphasis on the ophiostomatoid fungi. In: *Bark and Wood Boring Insects in Living Trees in Europe, a synthesis*. Kluwer Academic Publishers, Dordrecht, The Netherlands, pp. 181–235.

Klepzig KD, Adams AS, Handelsman J, Raffa KF, 2009. Symbioses: a key driver of insect physiological processes, ecological interactions, evolutionary diversification, and impacts on humans. *Environmental Entomology* **38**: 67–77.

Please cite this article in press as: Taerum SJ, et al., Putative origins of the fungus *Leptographium procerum*, Fungal Biology (2016), http://dx.doi.org/10.1016/j.funbio.2016.09.007

Kopelman NA, Mayzel J, Jakobsson M, Rosenberg NA, Mayrose I, 2015. CLUMPAK: a program for identifying clustering modes and packaging population structure inferences across K. *Molecular Ecology Resources* **15**: 1179–1191.

Larkin MA, Blackshields G, Brown NP, Chenna R, McGettigan PA, McWilliam H, Valentin F, Wallace IM, Wilm A, Lopez R, Thompson JD, Gibson TJ, Higgins DG, 2007. Clustal W and clustal X version 2.0. *Bioinformatics* **23**: 2947–2948.

Linnakoski R, de Beer ZW, Duong TA, Niemelä P, Pappinen A, Wingfield MJ, 2012. *Grosmannia* and *Leptographium* spp. associated with conifer-infesting bark beetle in Finland and Russia, including *Leptographium taigense* sp. nov. *Antonie van Leeuwenhoek* **102**: 375–399.

Loo JA, 2009. Ecological impacts of non-indigenous invasive fungi as forest pathogens. *Biological Invasions* **11**: 81–96.

Lou Q-Z, Lu M, Sun JH, 2014. Yeast diversity associated with invasive *Dendroctonus valens* killing *Pinus tabuliformis* in China using culturing and molecular methods. *Microbial Ecology* **68**: 397–415.

Lu M, Zhou XD, de Beer ZW, Wingfield MJ, Sun JH, 2009a. Ophiostomatoid fungi associated with the invasive pine-infesting bark beetle, *Dendroctonus valens*, in China. *Fungal Diversity* **38**: 133–145.

Lu Q, Decock C, Zhang XY, Maraite H, 2009b. Ophiostomatoid fungi (Ascomycota) associated with *Pinus tabuliformis* infested by *Dendroctonus valens* (Coleoptera) in northern China and an assessment of their pathogenicity on mature trees. *Antonie van Leeuwenhoek* **96**: 275–293.

Lu M, Wingfield MJ, Gillette NE, Mori SR, Sun JH, 2010. Complex interactions among host pines and fungi vectored by an invasive bark beetle. *The New Phytologist* **187**: 859–866.

Lu M, Wingfield MJ, Gillette NE, Sun JH, 2011. Do novel genotypes drive the success of an invasive bark beetle-fungus complex? Implications for potential reinvasion. *Ecology* **92**: 2013–2019.

Masuya H, Yamaoka Y, Wingfield MJ, 2013. Ophiostomatoid fungi and their associations with bark beetles in Japan. In: Seifert KA, de Beer ZW, Wingfield MJ (eds), *The Ophiostomatoid Fungi: expanding frontiers*. CBS-KNAW Fungal Biodiversity Centre, Utrecht, The Netherlands, pp. 77–90.

Möller EM, Bahnweg G, Sandermann H, Geiger HH, 1992. A simple and efficient protocol for isolation of high-molecular-weight DNA from filamentous fungi, fruit bodies, and infected-plant tissues. *Nucleic Acids Research* **20**: 6115–6116.

Mueller UG, Gerardo NM, Aanen DK, Six DL, Schultz TR, 2005. The evolution of agriculture in insects. *Annual Review of Ecology, Evolution and Systematics* **36**: 563–595.

Nei M, 1973. Analysis of gene diversity in subdivided populations. *Proceedings of the National Academy of Sciences of the United States of America* **70**: 3321–3323.

Owen DR, Smith SL, Seybold SJ, 2010. *Red turpentine beetle* U.S. Department of Agriculture, Forest Pest Leaflet 55.

Palm ME, 2001. Systematics and the impact of invasive fungi on agriculture in the United States. *Bioscience* **51**: 141–147.

Peakall R, Smouse PE, 2012. GenAlEx 6.5: genetic analysis in Excel. Population genetic software for teaching and research – an update. *Bioinformatics* **28**: 2537–2539.

Piou D, 1993. Possible role of *Hylobius abietis* (L) in the transport of *Leptographium procerum* (Kendr.) Wingf. and in the infection of Scots pine. *Annals of Forest Science* **50**: 297–308.

Ploetz RC, Hulcr J, Wingfield MJ, de Beer ZW, 2013. Destructive tree diseases associated with ambrosia and bark beetles: black swan events in tree pathology? *Plant Disease* **97**: 856–872.

Pritchard JK, Stephens M, Donnelly P, 2000. Inference of population structure using multilocus genotype data. *Genetics* **155**: 945–959.

Raffa KF, Aukema BH, Bentz BJ, Carroll AL, Hicke JA, Turner MG, Romme WH, 2008. Cross-scale drivers of natural disturbances prone to anthropogenic amplification: the dynamics of bark beetle eruptions. *Bioscience* **58**: 501–517.

Reay SD, Thwaites JM, Farrell RL, 2005. A survey of *Ophiostoma* species vectored by *Hylastesater* to pine seedlings in New Zealand. *Forest Pathology* **35**: 105–113.

Rosenberg NA, 2004. DISTRUCT: a program for the graphical display of population structure. *Molecular Ecology Notes* **4**: 137–138.

Sakai AK, Allendorf FW, Holt JS, Lodge DM, Molofsky J, With KS, Baughman S, Cabin RJ, Cohen JE, Ellstrand NC, McCauley DE, O'Neil P, Parker IM, Thompson JN, Weller SG, 2001. The population biology of invasive species. *Annual Review of Ecology and Systematics* **32**: 305–332.

Sun J, Lu M, Gillette NE, Wingfield MJ, 2013. Red turpentine beetle: innocuous native becomes invasive tree killer in China. *Annual Reviews of Entomology* **58**: 293–311.

Szpiech ZA, Jakobsson M, Rosenberg NA, 2008. ADZE: a rarefaction approach for counting alleles private to combinations of populations. *Bioinformatics* **24**: 2498–2504.

Taerum SJ, Konečný A, de Beer ZW, Cibrián-Tovar D, Wingfield MJ, 2016. Population genetics and symbiont assemblages support different invasion scenarios for the red turpentine beetle (*Dendroctonus valens*). *Biological Journal of Linnean Society London*. http://dx.doi.org/10.1111/bij.12781.

Taerum SJ, Duong TA, de Beer ZW, Gillette N, Sun JH, Owen DR, Wingfield MJ, 2013. Large shift in symbiont assemblage in the invasive red turpentine beetle. *PLoS One* **8**: e78126.

Tamura K, Peterson D, Peterson N, Stecher G, Nei M, Kumar S, 2011. MEGA5: molecular evolutionary genetics analysis using maximum likelihood, evolutionary distance, and maximum parsimony methods. *Molecular Biology and Evolution* **28**: 2731–2739.

van der Nest MA, Beirn LA, Crouch JA, Demers JE, de Beer ZW, De Vos L, Gordon TR, Moncalvo J-M, Naidoo K, Sanchez-Ramirez S, Roodt D, Santana QC, Slinski SL, Stata M, Taerum SJ, Wilken PM, Wilson AM, Wingfield MJ, Wingfield BD, 2014. Draft genomes of *Amanita jacksonii, Ceratocystis albifundus, Fusariumcircinatum, Huntiella omanensis, Leptographium procerum, Rutstroemiasydowiana*, and *Sclerotinia echinophila*. *IMA Fungus* **5**: 473–486.

Wang B, Salcedo C, Lu M, Sun JH, 2012. Mutual interactions between an invasive bark beetle and its associated fungi. *Bulletin of Entomological Research* **102**: 71–77.

Wanyera R, Kinyua MG, Jin Y, Singh RP, 2006. The spread of stem rust caused by *Puccinia graminis* f. sp *tritici*, with virulence on Sr31 in wheat in Eastern Africa. *Plant Disease* **90** 113–113.

Wingfield MJ, Capretti P, MacKenzie M, 1988. *Leptographium* spp. as root pathogens of conifers. An international perspective. In: Harrington TC, Cobb Jr FW (eds), *Leptographium Root Diseases on Conifers*. APS Press, St. Paul, Minnesota, pp. 113–128.

Wingfield MJ, Gibbs JN, 1991. *Leptographium* and *Graphium* species associated with pine-infesting bark beetles in England. *Mycological Research* **95**: 1257–1260.

Wingfield MJ, Seifert KA, Webber JF, 1993. Ceratocystis *and* Ophiostoma: *taxonomy, ecology, and pathogenicity*. APS Press, St. Paul, Minnesota.

Wingfield MJ, Slippers B, Wingfield BD, 2010. Novel associations between pathogens, insects and tree species threaten world forests. *New Zealand Journal of Forest Science* **40**: S95–S104.

Wingfield MJ, Garnas JR, Hajek A, Hurley BP, de Beer ZW, Taerum SJ, 2016. Novel and co-evolved associations between insects and microorganisms as drivers of forest pestilence. *Biological Invasions* **18**: 1045–1056.

Yan ZL, Sun JH, Don O, Zhang ZN, 2005. The red turpentine beetle, *Dendroctonus valens* LeConte (Scolytidae): an exotic invasive

pest of pine in China. *Biodiversity and Conservation* **14**: 1735–1760.

Yeh F, Yang R-C, Boyle T, Ye Z-H, Mao J, 1997. *POPGENE: the user-friendly shareware for population genetic analysis*. Molecular Biology and Biotechnology Centre, University of Alberta, Canada. http://www.ualberta.ca/~fyeh/.

Yin M, Duong TA, Wingfield MJ, Zhou XD, de Beer ZW, 2015. Taxonomy and phylogeny of the *Leptographium procerum* complex, including two new species from China and Japan. *Antonie van Leeuwenhoek* **107**: 547–563.

Zhang H, Geller JB, Vrijenhoek RC, 2014. Genetic diversity in native and introduced populations of the amethyst gem clam *Gemma gemma* (Totten, 1834) from the U.S. east and west coasts. *Biological Invasions* **16**: 2725–2735.

Zhou XD, de Beer ZW, Wingfield MJ, 2013. Ophiostomatoid fungi associated with conifer-infesting bark beetles in China. In: Seifert KA, de Beer ZW, Wingfield MJ (eds), *The Ophiostomatoid Fungi: expanding frontiers*. CBS-KNAW Biodiversity Centre, Utrecht, The Netherlands, pp. 93–100.

Please cite this article in press as: Taerum SJ, et al., Putative origins of the fungus *Leptographium procerum*, Fungal Biology (2016), http://dx.doi.org/10.1016/j.funbio.2016.09.007